

Heat Capacity of ^3He in Aerogel

Jizhong He, A.D. Corwin, J.M. Parpia, J.D. Reppy

Laboratory of Atomic and Solid State Physics and the Cornell Center for Material Research, Cornell University, Ithaca, NY 14853-2501

(December 2, 2024)

The heat capacity of pure ^3He in low density aerogel is measured at 22.5 bar. The superfluid response is simultaneously monitored with a torsional oscillator. A slightly rounded heat capacity peak, 70 μK in width, is observed at the aerogel- ^3He superfluid transition, T_{ca} . Subtracting the bulk ^3He contribution, the heat capacity shows a Fermi-liquid form above T_{ca} . The heat capacity attributed to superfluid within the aerogel can be fit with a rounded BCS form, and accounts for 0.28 of the non-bulk fluid in the aerogel, indicating a substantial reduction in the superfluid order parameter consistent with earlier superfluid density measurements.

The discovery of the superfluid transition of ^3He in aerogel glass in 1995 [1] [2], has aroused wide interest. The ^3He -aerogel system presents a unique opportunity for study of the influence of quenched impurities on the well-understood system of pure superfluid ^3He . Studies employing media such as sintered silver or packed powders [3] [4] were dominated by surface scattering and finite size effects [5]. Aerogel consists of a fractal structure of relatively uniform silica strands 30 \AA in diameter. In the case of 97.6% open aerogel, employed in the present experiment, scattering due to the silica strands is sufficiently weak so that, although the superfluid properties are modified, superfluidity is not strongly suppressed as it would be the case of more dense aerogel systems or packed powders. While previous measurements exposed the onset of superfluidity using NMR [2] [6] [7] [8] and acoustic techniques [9] [10], they could not distinguish between a percolation transition, where the flow and the specific heat anomaly are distinct, and a suppressed superfluid transition [11].

In the work presented here, we examined the ^3He superfluid state in aerogel through heat capacity measurements made at a pressure of 22.5 bar. Our chief result is the observation of a feature in the heat capacity coincident with the onset of superflow in the aerogel- ^3He system. This observation confirms that superflow onset corresponds to a true phase transition rather than to a possible dynamic effect associated with a percolation transition involving distributed superfluid regions. In earlier work [12], we reported on measurements of the heat capacity employing a drift technique. Those measurements gave an indication of an anomaly at the aerogel superfluid transition; however, a definitive resolution of this peak has required the experimental improvements of the present experiment.

In Fig. 1, we show a cut-away diagram of the latest version of our heat capacity apparatus. The cell containing the ^3He -aerogel sample also forms the inertial head of

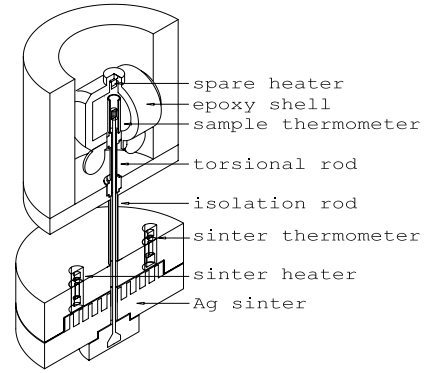


FIG. 1. A cross-section of the experimental cell is shown.

a torsional oscillator. We are thus able to correlate features in the heat capacity with the dynamic superfluid response. The liquid ^3He within the apparatus is cooled by a silver sinter pad, which is in turn bolted for thermal contact to a PrNi_5 nuclear cooling stage. There are two lanthanum diluted cerium magnesium nitrate (LCMN) thermometers; one inside the sample cell and the other located in the region of the silver sinter. These are operated in a dc mode similar to that of the SQUID based thermometer developed by Lipa and Chui [13]. Thermometer calibration is provided by comparison to a melting curve thermometer mounted on the nuclear cooling stage [14]. Thermal contact between the heat capacity cell and the cooling stage is established via the ^3He contained in the hollow torsion rod connecting the heat capacity cell to the stage. The time constant associated with this thermal contact path is designed to be at least an order of magnitude longer than the internal thermal relaxation time within the heat capacity cell itself. Heat pulses are

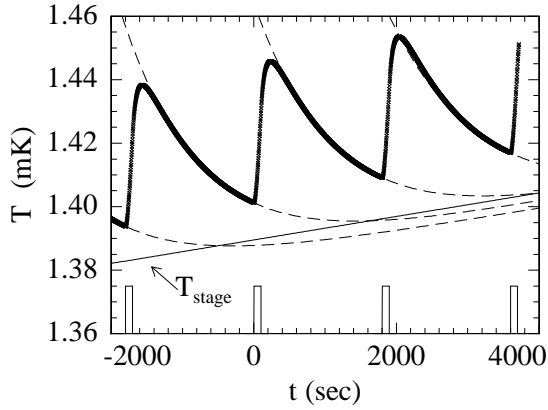


FIG. 2. The thermal response of the cell thermometer to a series of four heat pulses at 1800 second intervals is shown as a function of time. The timing of the heat pulses is indicated schematically at the bottom of the figure. The solid line indicates the steady drift of the stage temperature and the dashed curves are fits of the exponential decay function (see text) to the relaxation portion of the cell thermal response following a heat pulse.

applied to the sample by a non-inductive resistive heater wound around the aerogel sample. Care is taken that the heater is not close to the LCMN thermometer. In addition, a second spare heater, shown in Fig. 1, was placed in the cell.

Our measurement technique is illustrated in Fig. 2. Following a demagnetization to our lowest temperatures, the cell warms slowly over a period of several days. During this warming interval, a sequence of heat pulses is applied to the ^3He within the cell and the heat capacity is determined as a function of temperature. Representative data is shown in Fig. 2, where a series of successive heat pulses and the subsequent thermal relaxation of the sample cell temperature, $T_c(t)$, is shown. In this example, the stage temperature $T_s(t)$, is increasing at a steady rate of $15.6 \mu\text{K/hr}$ and identical heat pulses are repeated at 1800 second intervals. Following each heat pulse, the cell temperature rises rapidly. Initially the temperature distribution within the cell is nonuniform. The internal equilibrium time is relatively short and therefore at longer times the thermal distribution within the cell becomes nearly uniform and the cell temperature exhibits an exponential relaxation of the form, $T_c(t) = T_0 e^{-t/\tau} + T_s(t) - \alpha\tau$, where α is the warming rate of the stage and τ is the relaxation time constant. Fits of this exponential function to the relaxation portion of the thermal pulses are shown in the figure.

The temperature excursion during each heat pulse is relatively small, on the order of 40 to 50 μK . Therefore in our preliminary analysis we take the heat capacity, C , and thermal conductivity, κ , to be constant over the period of each relaxation. We proceed by calculating the net energy flow, Q , into or out of the cell during a time

interval, t_1 to t_2 . We restrict these times to the exponential portion of the cell's thermal relaxation. During this period the LCMN thermometer gives a reliable value for the temperature throughout the cell. The energy flow from the cell due to thermal conduction down the torsion rod to the stage is then obtained by numerical integration of the quantity $\kappa(T_c(t) - T_s(t))$, over the chosen time interval. If the time interval contains the heat pulse, we include the energy, Q_{in} , contributed by the heater. A possible choice for the first time interval would be to take $t_1 = 0$, the time just before the heat pulse, and $t_2 = t_f$, the time at the end of the relaxation period just before the next heat pulse. The second interval, which will not include a heat pulse, might start at time t (chosen in the exponential decay region) and ends at t_f as for the first interval. Then we write two independent equations containing the heat capacity and the thermal conductivity.

$$C(T_c(t_f) - T_c(0)) = Q_{in} - \kappa \int_0^{t_f} (T_c(t) - T_s(t)) dt \quad (1)$$

$$C(T_c(t_f) - T_c(t)) = -\kappa \int_t^{t_f} (T_c(t) - T_s(t)) dt \quad (2)$$

These equations are then solved for C and κ with A defined as $\int_0^t (T_c(t) - T_s(t)) dt$ and A_f defined as $\int_0^{t_f} (T_c(t) - T_s(t)) dt$.

$$C(t) = \frac{(A_f - A)Q}{A_f(T_c(t) - T_c(0)) - A(T_c(t_f) - T_c(0))} \quad (3)$$

$$\kappa(t) = \frac{(T_c(t) - T_c(t_f))Q}{A_f(T_c(t) - T_c(0)) - A(T_c(t_f) - T_c(0))} \quad (4)$$

One advantage of this approach is that one can vary t , and check that the calculated values for C and κ are not sensitive to this choice. The thermal conductivity obtained from the above analysis is found to be a smoothly varying function of temperature except at the bulk superfluid transition where the conductivity drops by over a factor of two as the temperature rises through the transition temperature. A more detailed discussion of the data analysis and the cell construction will be found elsewhere [15] [16].

In Fig. 3, we have plotted the total heat capacity determined for temperatures between 0.6 to 4 mK. We also show the Q^{-1} for the torsional oscillator. There are two conspicuous features in the heat capacity data. The first is the heat capacity anomaly associated with the superfluid transition in the ^3He -aerogel sample, which coincides with the superfluid aerogel transition, T_{ca} , as marked by the torsional oscillator. The second feature is the sharp jump in the heat capacity due to bulk ^3He within the cell. Above the bulk transition, T_{c0} , a linear temperature dependence is seen as expected for a normal

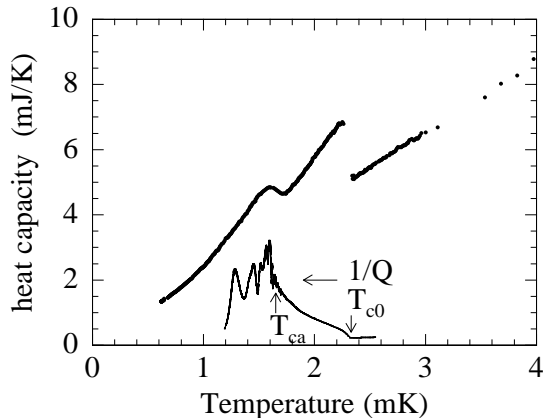


FIG. 3. The total measured heat capacity for the ^3He -aerogel sample at a pressure of 22.5 bar is shown as a function of temperature. The dissipation, Q^{-1} , of the torsional oscillator is also shown. The bulk superfluid transition, T_{c0} , and the ^3He in aerogel transition, T_{ca} , are clearly indicated in the $1/Q$ response.

Fermi liquid. We also note that in addition to the linear term in this region there appears to be a small additional constant contribution to the heat capacity ($\approx 10\mu\text{J/K}$). Golov and Pobell suggest that this contribution may arise from ordering in the amorphous solid ^3He layer [17].

Since our main interest is in the heat capacity associated with the ^3He -aerogel superfluid transition, we shall subtract the bulk ^3He heat capacity contribution. For this purpose we have used the data of Greywall [14] and multiply by a suitable factor so as to produce a smooth continuation of the remaining heat capacity data across the temperature of the bulk transition. The magnitude of the subtracted heat capacity indicates that a fraction (0.295) of the sample has the heat capacity of bulk ^3He . This fraction is more than we can reasonably account for in terms of cracks and small volumes outside of the aerogel itself. Therefore we conclude that our sample of aerogel must contain a number of macroscopic pores.

The heat capacity data remaining after the subtraction of the bulk are shown in Fig. 4. The heat capacity anomaly associated with the aerogel transition shows rounding but is clearly separated from the bulk transition. The linear Fermi liquid region extends smoothly from temperatures above the bulk transition right to the aerogel transition. In the region between the bulk transition and the aerogel T_c we find no indications of anomalous behavior such as might be suggested by recent Grenoble NMR experiments [8].

The ^3He in aerogel effective mass, m_a^* , can be determined from the slope of the heat capacity in the Fermi-liquid region [14] [19] after the fraction of bulk ^3He has been subtracted. From the data of Fig. 4, we find $m_a^*/m = 6.5$, approximately 30 % larger than the ratio for bulk superfluid ^3He at this pressure. This is not

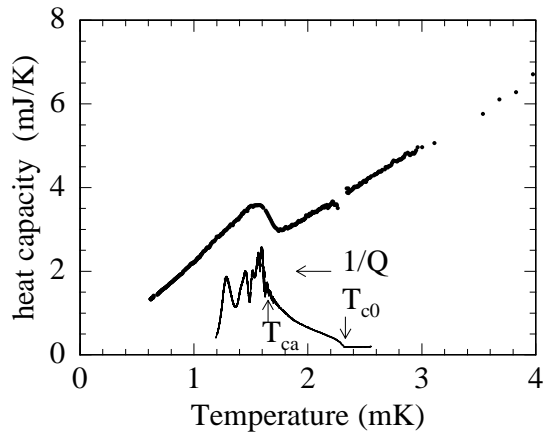


FIG. 4. The heat capacity remaining after the subtraction of the bulk contribution is shown as a function of temperature.

surprising since the extremely low density aerogel has been predicted to have little influence on the Fermi-liquid properties of the pure liquid [18]. Above the superfluid transition the chief effect of the aerogel is to reduce the mean free path of the quasiparticles.

The simplest theoretical approach to the problem of superfluid ^3He in aerogel is that of the Homogeneous Scattering Model (HSM) [18], which treats the aerogel as homogeneous collection of scattering centers. The HSM predicts a reduction of the transition temperature comparable to that seen in the experiments as well as suppression of the order parameter.

In order to assess the fraction of fluid, f_a , contributing to the aerogel superfluid transition, we have fit the data to a BCS form (Eq. 5). We take the bulk value for the gap, Δ , a transition temperature, T_{ca} , of 1.65 mK, the normal fermi liquid heat capacity contribution, $C_n(T_{ca})$, and the exponent a as a fitting parameter on the order of unity.

$$C_s(T) = C_n(T_{ca})f_a(1 + \Delta)e^{-a(T_{ca}/T-1)} \quad (5)$$

Since the peak in the heat capacity is somewhat rounded we convolve this BCS form with a gaussian function. Following a procedure similar to that used to obtain the data shown in Fig.4, we subtract a heat capacity of the BCS form from the data shown in Fig.4. The width of the gaussian ($70\mu\text{K}$) is adjusted to produce a remainder that is smooth through the region near T_{ca} . The results of this procedure are shown in Fig. 5. The heat capacity anomaly at T_{ca} has been removed by this procedure. The quantity subtracted is shown as a solid line in the figure. Somewhat surprisingly, we find that the fraction of the fluid that appears to participate in the aerogel superfluid state is only a fraction 0.28 of the total. Expressed in terms of the order parameter, one would conclude that there has been a reduction by a factor of over two-thirds under the conditions of our experiment. This result is in

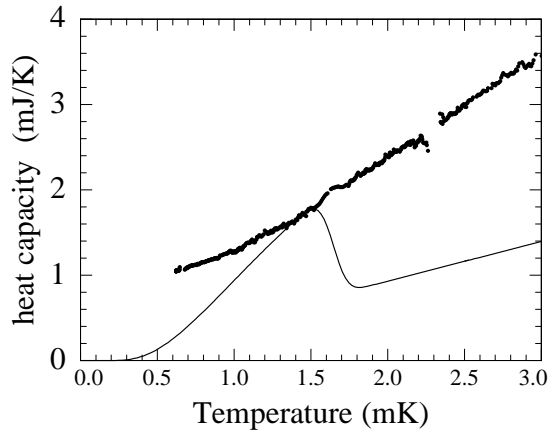


FIG. 5. The normal Fermi liquid in the aerogel seen after subtracting a BCS-like superfluid transition at T_{ca} (shown as the solid line). Note the upturn at lowest temperatures, suggesting magnetic ordering

keeping with the order parameter reductions observed in the Cornell torsional oscillator experiments [1].

The striking feature of Fig. 5 is that 72% of the fluid in the aerogel (after the subtraction of the bulk contribution) exhibits a linear Fermi-liquid-like temperature dependence down to the lowest temperatures. There is however, an additional upturn in the remaining heat capacity at low temperatures. This might be expected as a consequence of the magnetic ordering of the solid ^3He substrate atoms. Such an ordering of the solid layer is a feature observed in the earlier NMR aerogel experiments [2] [6] [7]. As has been demonstrated in the NMR [6], the magnetic influence of the solid ^3He layer can be removed by the addition of a few layers of ^4He on the substrate. This will be an interesting direction to pursue in future aerogel heat capacity experiments.

In conclusion, we find that the behavior of ^3He confined to aerogel shows normal Fermi liquid characteristics both above and below the superfluid transitions. While a sizeable fraction of fluid in the cell exhibits bulk like characteristics, a comparable fraction displays a BCS like heat capacity centered at the reduced T_c , in conformity with expectations of a suppressed phase transition. We find that the magnitude of the order parameter is reduced by an amount comparable to that observed in torsional pendulum measurements [1]. Evidence for magnetic order in this system can also be qualitatively inferred from the residual heat capacity below the superfluid transition.

The authors are especially grateful to Prof. Norbert Mulders of the University of Delaware who supplied the aerogel sample used in this experiment. We also acknowledge valuable discussions with Prof.'s M.H.W. Chan, T.L. Ho, and Dr. E.N. Smith. One of us, J.D.R. would like to acknowledge the Institute for Solid State Physics, University of Tokyo, for hospitality during the period this paper was prepared. The research has been funded by the

-
- [1] J.V. Porto and J.M. Parpia, Phys. Rev. Lett. **74**, 4667 (1995).
 - [2] D.T. Sprague, T.M. Haard, J.B. Kycia, M.R. Rand, Y. Lee, P.J. Hamot, and W.P. Halperin, Phys. Rev. Lett. **75**, 661 (1995).
 - [3] T. Hall, S.M. Tholen, K.R. Lane, V. Kotsubo, and J.M. Parpia, J. Low Temp. Phys. **89**, 897 (1992).
 - [4] K. Ichikawa, S. Yamasaki, H. Akimoto, T. Kodama, T. Shigi, and H. Kojima, Phys. Rev. Lett. **58**, 1949 (1987).
 - [5] V. Ambegaokar, P.G. de Gennes, and D. Rainer, Phys. Rev. A **9** 2676 (1974).
 - [6] H. Alles, J.J. Kaplinsky, P.S. Wootton, J.D. Reppy, J.H. Naish, and J.R. Hook, Phys. Rev. Lett. **83**, 1367 (1999).
 - [7] B.I. Barker, Y. Lee, L. Polukhina, D.D. Osheroff, L.W. Hrubesh, and J.F. Poco, Phys. Rev. Lett. **85**, 2148 (2000).
 - [8] Y.M. Bunkov, A.S. Chen, D.J. Cousins, and H. Godfrin, Phys. Rev. Lett. **85**, 3456 (2000).
 - [9] A. Golov, D.A. Geller, J.M. Parpia, and N. Mulders, Phys. Rev. Lett. **82**, 3492 (1999).
 - [10] G. Gervais, K. Yawata, N. Mulders, and W.P. Halperin, `cond-matt/0202323` unpublished.
 - [11] C. Ebner, and D. Stroud, Phys. Rev. B **23** 6164 (1981).
 - [12] Jizhong He, A.D. Corwin, G.M. Zassenhaus, A.L. Woodcraft, N. Mulders, J.M. Parpia, J.D. Reppy, and M.H.W. Chan, J. Low Temp. Phys. **121**, 561 (2000).
 - [13] J.A. Lipa, B.C. Leslie, and T.C. Wallstrom. Proceedings of LT-16 in *Physica* **107B**, 331 (1981); T.C.P. Chui and J.A. Lipa, Proc. LT-17, U. Eckern, A. Schmid, W. Weber, H. Wuhl eds., North-Holland Amsterdam, 931 (1984).
 - [14] D.S. Greywall, Phys. Rev. B **33**, 7520 (1986).
 - [15] Jizhong He, A.D. Corwin, N. Mulders, J.M. Parpia, J.D. Reppy, and M.H.W. Chan, J. Low Temp. Phys. **126**, 679 (2002).
 - [16] A.D. Corwin, Cornell University Ph. D. Thesis, 2002 unpublished.
 - [17] A. Golov, and F. Pobell, Phys. Rev. B **53**, 12647 (1996).
 - [18] E.V. Thuneberg, S.K. Yip, M. Fogelstrom, and J.A. Sauls, Phys. Rev. Lett. **80**, 2861 (1998).
 - [19] J.C. Wheatley, Rev. Mod. Phys. **47**, 415 (1975).